ChemComm

Cite this: *Chem. Commun.*, 2011, **47**, 12107–12109

www.rsc.org/chemcomm

COMMUNICATION

Signal amplification by adsorption-induced catalytic reduction of dissolved oxygen on nitrogen-doped carbon nanotubes for electrochemiluminescent immunoassay†

Shengyuan Deng,[a] Zhentao Hou,[a] Jianping Lei,[a] Dajie Lin,[a] Zheng Hu,[b] Feng Yan[c] and Huangxian Ju*[a]

Received 18th September 2011, Accepted 5th October 2011
DOI: 10.1039/c1cc15766c

A signal amplification strategy was proposed for quantum dot-based electrochemiluminescence by an adsorption-induced catalytic reduction of dissolved oxygen at the sidewall of nitrogen-doped carbon nanotubes, which led to a 'signal-on' sandwich immunoassay with a linear range of 6 orders of magnitude.

Electrochemiluminescence (ECL) is a sensitive technique integrating the advantages of electrochemistry and chemiluminescence.[1] The quantum dots (QDs)-based ECL, which is usually generated in annihilation and coreactant routines, has attracted broad research interest.[2] Various mechanisms have been proposed for coreactant-induced ECL emission.[2] Upon the elucidation of the ECL mechanisms, these ECL systems have also been utilized for development of different analytical methodologies.

To promote the ECL emission efficiency, functional nanomaterials have been introduced into QDs-based ECL systems to achieve good analytical performance, such as carbon nanotubes (CNTs) and graphene, which are normally employed as substrates to improve the ECL emission of QDs.[3] Compared with conventional CNTs, heterodoped nanotubes especially NCNTs are now extremely attractive because the association of nitrogen lone-pair electrons with the graphene π-conjugation may emerge novel nanomaterials with tailored chemophysical properties.[4] The nitrogen-induced charge delocalization at NCNTs can change the chemisorption mode of O_2 from the usual monoatomic end-on adsorption at CNTs to a diatomic side-on adsorption at sidewalls, which effectively weakens the O–O bonding to facilitate the reduction of O_2.[4] Furthermore, the doped N atoms can accelerate the kinetics of the initial reduction of O_2 to the intermediate superoxide ($O_2^{\bullet -}$) in the oxygen reduction reaction,[5] which may potentially provide a novel ECL mechanism using $O_2^{\bullet -}$ as the coreactant of QDs-based ECL.

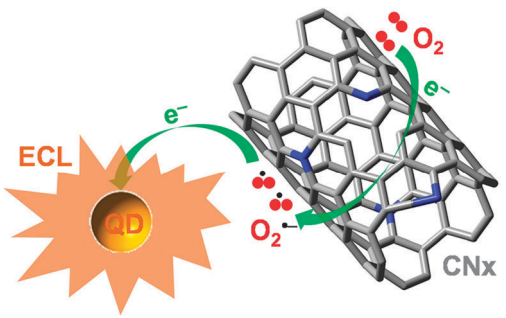

Scheme 1 An enhanced ECL emission mode *via* the adsorption-induced electron transfer of dissolved O_2 on NCNT.

Here the adsorption-induced catalytic reduction of dissolved O_2 at the sidewall of NCNTs was proposed to electrochemically produce $O_2^{\bullet -}$ for promoting the ECL emission of QDs (Scheme 1). The NCNTs were introduced to a QDs-based immunosensor to perform the new ECL amplification process by functionalizing the NCNTs with polystyrene sulfonate (PSS) for labeling signal antibody (Ab_2) and forming a sandwich immunocomplex on QDs and a capture antibody (Ab_1) modified electrode. The intrinsic strong adsorption of dissolved O_2 on NCNTs induced the electrochemical reduction of O_2 accompanying with the catalysis of NCNTs to produce $O_2^{\bullet -}$, which accelerated the kinetics of the ECL reaction. Thus a sensitive 'signal-on' ECL immunosensing method was developed without the need of a strong oxidant as coreactant. The 'signal-on' method could decrease the false positive usually occurring in 'signal-off' ECL immunosensing methods based on the steric hindrance resulting from the formation of immunocomplex and the consumption of the ECL coreactant in an enzymatic reaction.[6] The use of NCNTs as a label in QDs-based ECL could also avoid blackbody effect.[3a]

The as-prepared CdS QDs were characterized by UV-vis and PL spectra (Fig. S1 in ESI†). As shown in Fig. 1A, curve a, the water-soluble CdS QDs modified glassy carbon electrode (GCE) could be reduced in oxygen-free pH 8.0 PBS to generate a cathodic wave starting at −0.94 V with a peak at −1.36 V, suggesting that the anion radical $QD^{\bullet -}$ could directly be

[a] *State Key Laboratory of Analytical Chemistry for Life Science, Nanjing University, P.R. China. E-mail: hxju@nju.edu.cn*
[b] *Key Laboratory of Mesoscopic Chemistry (Ministry of Education of China), Department of Chemistry, Nanjing University, Nanjing 210093, P.R. China*
[c] *Jiangsu Institute of Cancer Prevention and Cure, Nanjing 210009, P.R. China*

† Electronic supplementary information (ESI) available: Experimental details, spectroscopic and morphology characterization, optimal conditions and sensing performance. See DOI: 10.1039/c1cc15766c

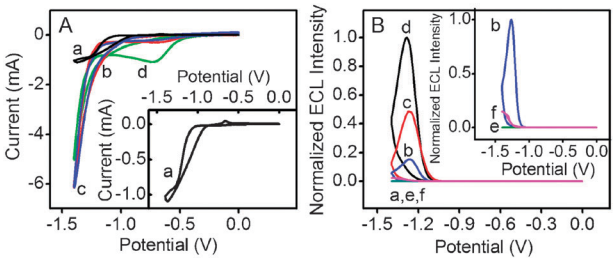

Fig. 1 (A) Cyclic voltammograms and (B) ECL-potential curves of CdS QDs modified GCE in N_2-saturated (a), air-saturated (b), 320 μM H_2O_2 + N_2-saturated (c), O_2-saturated (d), 1 mM L-cysteine + air-saturated (e) and 0.2 mg mL^{-1} SOD + air-saturated (f) 0.1 M pH 8.0 PBS. Insets in (A and B) magnified curve (a) and ECL-potential curves (b), (e) and (f).

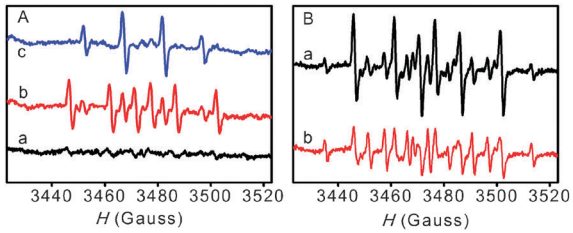

Fig. 2 (A) EPR spectra of deaerated pH 8.0 PBS containing 50 mM DMPO (a), and 0.1 M pH 8.0 PBS containing 60 μM O_2 and 50 mM DMPO recorded after applying the potential of −0.8 (b) and −1.8 V (c) on QDs modified GCE for 150 s. (B) EPR spectra of 0.1 M pH 8.0 PBS containing 60 μM O_2 and 50 mM DMPO recorded after applying a potential of −0.8 V on PNCNTs (a) and PCNTs (b) modified GCE for 150 s. The EPR signal was obtained with an accumulation of five cycles.

produced from the electro-reduction of QD at –0.94 V by an electron injection. In air- and O_2-saturated pH 8.0 PBS, the QDs film showed a reduction wave with an onset potential of about −0.47 V and peaked at −0.71 V, which could be attributed to the reduction of dissolved O_2 at the QDs film (Fig. 1A, curve b).

Fig. 1B shows the discrepancy of ECL signals enhanced by O_2 and H_2O_2 by immersing the QDs film in the O_2-saturated (Fig. 1B, curve d) or deaerated detection solution containing 320 μM H_2O_2 (Fig. 1B, curve c), which approximates the saturated concentration of dissolved O_2 at room temperature under standard atmospheric pressure.[7a] The QDs-based ECL peak intensity in O_2-saturated PBS was twice that in N_2-saturated PBS containing 320 μM H_2O_2. Thus the dissolved O_2 is a more efficient coreactant to enhance the ECL emission of QDs. After the detection solution was bubbled with highly pure N_2 for 30 min, the cathodic ECL emission disappeared (Fig. 1B, curve a). Furthermore, the introduction of 1 mM L-cysteine into the air-saturated detection solution could completely quench the ECL emission (Fig. 1B, curve e) as L-cysteine is an efficient scavenger of both hydroxyl and superoxide radicals.[7b] When superoxide dismutase (SOD) was introduced into the air-saturated solution, the ECL response also showed an 85% decrease (Fig. 1B, curve f) due to its specificity to annihilate superoxide with a rate constant up to 10^9 M^{-1} s^{-1}, indicating that the ECL emission was possibly related to $O_2^{\bullet-}$ species produced from the dissolved oxygen.

To verify the formation of intermediate $O_2^{\bullet-}$ at the modified GCE, electron paramagnetic resonance (EPR) spectra were used to record the process in tandem. Before the electrochemical process, the deaerated pH 8.0 PBS containing 50 mM 5,5-dimethyl-1-pyrroline N-oxide (DMPO) as the spin trap did not show any obvious signal (Fig. 2A, curve a). After a potential of –0.8 V was applied on the QDs modified electrode in pH 8.0 PBS containing 60 μM dissolved O_2 and 50 mM DMPO for 150 s, six sharp hyperfine split peaks emerged at 3448, 3463, 3473, 3479, 3488 and 3503 G (Fig. 2A, curve b), which entirely corresponded to the characteristics of the DMPO–$O_2^{\bullet-}$ adducts,[8] verifying the presence of superoxide radical in this system. Thus, the electrochemical process initiated the conversion of O_2 into superoxide at the QDs modified electrode.

Another batch of four relatively weak signals appeared at 3453, 3468, 3483 and 3498 G with an intensity ratio of 1 : 2 : 2 : 1, indicating the existence of hydroxyl radicals at such a potential. This result is consistent with Fig. 1B, curve f, in which the addition of sufficient SOD (0.2 mg mL^{-1}) did not totally annihilate the ECL emission, suggesting the coexistence of hydroxyl and superoxide radicals. After continuous potentiostatic electrolysis at −1.8 V for 150 s, the EPR peaks corresponding to $O_2^{\bullet-}$ disappeared while $OH^{\bullet}$ was distinguished and did not show any Gauss displacement (Fig. 2A, curve c). Thus, $OH^{\bullet}$ may be produced by the electrochemical reduction of $O_2^{\bullet-}$ at rather negative potential.[9] The EPR characterization further validated that the main participant of dissolved O_2 in the QDs-based ECL was $O_2^{\bullet-}$ produced from the following reaction at the electrode surface:

$$O_2 + e^- \rightarrow O_2^{\bullet-} \quad (1)$$

After applying a potential of −0.8 V on PNCNTs modified GCE, the EPR spectrum exhibited six distinguishable hyperfine split peaks at 3447, 3462, 3472, 3478, 3487 and 3503 G, which are the characteristic EPR spectral of $O_2^{\bullet-}$, while PCNT modified GCE exhibited only one third intensity of that of PNCNT (Fig. 2B), suggesting that more $O_2^{\bullet-}$ was generated at PNCNTs modified GCE. This result supported the conclusion that the strong adsorption ability of PNCNTs accelerates the reduction rate of O_2 at Ab_2-PNCNTs facilitating the formation of $O_2^{\bullet-}$.[5b]

The morphology of NCNTs and subsequent functionalizations were characterized and validated in Fig. S2 and S3 in ESI.† Fig. 3A depicts the electrochemical responses of Ab_2-PNCNTs modified GCE to different concentrations of dissolved O_2, which were prepared by precisely controlling the flow rate and time of pure O_2 into N_2-saturated buffer.

With the increasing O_2 concentration the cathodic peak current gradually increased and then tended to a maximum value, following a Langmuir-type adsorption isotherm.

$$c/i_{p,c} = c/(i_{p,c})_{max} + b - 1/(i_{p,c})_{max} \quad (2)$$

Evaluated from eqn (2), the adsorption equilibrium constant of O_2 at Ab_2-PNCNTs (4.33×10^3 L mol^{-1}) is nearly twice that at Ab_2-PCNTs (2.33×10^3 L mol^{-1}). This could be attributed to more edge plane sites of the NCNTs than the CNTs, assuming the amount of adsorbed O_2 is proportional to the degree of edge plane character.[5a] The strong adsorption

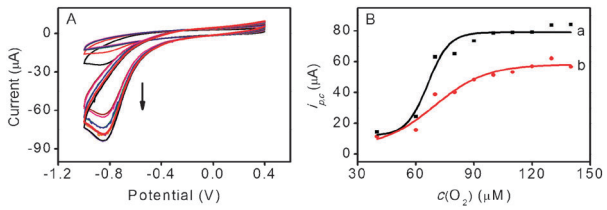

Fig. 3 (A) Cyclic voltammograms of Ab_2-PNCNTs modified GCE at different concentrations of O_2 in N_2-saturated 0.1 M pH 8.0 PBS at room temperature. (B) O_2 adsorption isotherms at Ab_2-PNCNTs (a) and Ab_2-PCNT (b) modified GCEs.

ability of PNCNTs led to adsorption-induced catalytic reduction of O_2 at Ab_2-PNCNTs.

Atomic force microscopic images (Fig. S3D–H in ESI†) and electrochemical impedance spectra (Fig. S4 in ESI†) were utilized to monitor the sequential fabrication of the QDs-based ECL immunosensor and the recognition of carcinoembryonic antigen (CEA) onto the immunosensor. The electron transfer resistance gradually increased due to the insulating properties of proteins. However, its value decreased from 5470 to 3960 Ω after Ab_2-PNCNTs were bound to the QDs/Ab_1/BSA/CEA surface to form the sandwich-typed immunocomplex, which further confirmed the role of NCNTs for improving the ECL emission of the immunosensor.

As shown in Fig. 4A, with the stepwise coverage of Ab_1, BSA and CEA on the QDs/chitosan modified electrode surface the ECL emission greatly decreased due to their nonconductive properties and steric hindrance. The increasing electron transfer resistance made the ECL peak potential progressively negatively shift from −1.2 to −1.3 V. Interestingly, after the Ab_2-PNCNTs were bound to QDs/Ab_1/BSA/CEA modified GCE, the ECL intensity increased by 130%. The increase extent was greater than the decrease extent of 27.6% for electron transfer resistance. Therefore, the promoted conversion rate of dissolved O_2 to superoxide by PNCNTs played a key role. Meanwhile, the increase extent was 1.9-times that by PCNTs, which was in consistent with the ratio of the adsorption equilibrium constant. The enhanced ECL response led to a new signal amplification strategy and a 'signal-on' immunoassay method.

Under the optimal conditions (Fig. S5 in ESI†), the ECL intensity of the immunosensor increased with the increasing concentration of CEA in the incubation solution (Fig. 4B). The calibration plot showed a good linear relationship between the ECL intensity and the logarithm value of CEA concentration in the range from 50 pg mL^{-1} to 5 μg mL^{-1} with a correlation coefficient of 0.993 (Fig. 4B, inset). The limit of detection at a signal-to-noise ratio of 3 was 2.4 pg mL^{-1}, which was at least 50 times lower than those previously reported by electrochemical immunoassay with different amplification strategies.[9] More importantly, this 'signal-on' immunoassay method showed a wide detection range of 6 orders of magnitude and avoided the need of deoxygenating for electrochemical immunoassay.

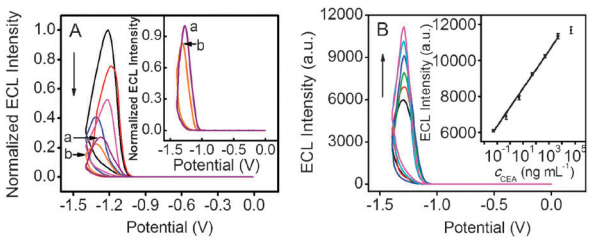

Fig. 4 (A) ECL-potential curves in air-saturated pH 8.0 PBS of QDs, QDs/Ab_1, QDs/Ab_1/BSA/CEA/Ab_2-PNCNTs, QDs/Ab_1/BSA and QDs/Ab_1/BSA/CEA/Ab_2-PCNTs, QDs/Ab_1/BSA/CEA modified GCE (from top to bottom). (B) ECL response of the immunosensor to 0.05, 0.5, 5, 50, 500 and 5000 ng mL^{-1} CEA (from bottom to top). Inset in (A) magnified curves of (a) and (b). Inset in (B) calibration curve.

The ECL immunosensor showed good stability and reproducibility (Fig. S6 in ESI†) and acceptable accuracy for serum samples assay (Table S1 in ESI†). Although the reusability is a drawback of the proposed sandwich format, the excellent repeatability and good accuracy made it possible for preparation of disposable immunosensors. Considering the CEA threshold of 5 ng mL^{-1} for clinical diagnosis,[10] the proposed method possessed good practicability.

In conclusion, a facile signal amplification strategy is developed for 'signal-on' immunoassay based on a novel ECL mechanism of QDs by adsorption-induced catalytic reduction of dissolved O_2 on NCNTs, which produces the superoxide radical to enhance the ECL emission. The NCNTs functionalized with polyelectrolyte show nearly twice stronger adsorption ability toward dissolved O_2 than CNTs, which leads to faster formation of superoxide radical and thus improves the ECL emission of the immunosensor. The proposed 'signal-on' ECL immunoassay method shows high sensitivity, good precision and acceptable accuracy along with a wide linear range up to 6 orders of magnitude. The functionalized NCNTs provide new opportunities in both exploring the new QDs-based ECL systems and expanding the new application avenues of carbon nanomaterials in bioassays.

This work was financially supported by the Important National S&T Specific Project (2009ZX10004-313), National Basic Research Program of China (2010CB732400) and National Natural Science Foundation of China (21135002 and 20875044).

Notes and references

1 M. M. Richter, *Chem. Rev.*, 2004, **104**, 3003–3036.
2 W. J. Miao, *Chem. Rev.*, 2008, **108**, 2506–2553.
3 (*a*) X. F. Wang, Y. Zhou, J. J. Xu and H. Y. Chen, *Adv. Funct. Mater.*, 2009, **19**, 1–7; (*b*) Y. S. Guo, X. P. Jia and S. S. Zhang, *Chem. Commun.*, 2011, **47**, 725–727.
4 K. P. Gong, F. Du, Z. H. Xia, M. Durstock and L. M. Dai, *Science*, 2009, **323**, 760–764.
5 (*a*) J. L. Lyon and K. J. Stevenson, *Electrochim. Acta*, 2008, **53**, 6714–6721; (*b*) S. Maldonado and K. J. Stevenson, *J. Phys. Chem. B*, 2004, **108**, 11375–11383.
6 J. P. Lei and H. X. Ju, *TrAC, Trends Anal. Chem.*, 2011, **30**, 1351–1359.
7 (*a*) H. Jiang and H. X. Ju, *Chem. Commun.*, 2007, 404–406; (*b*) H. Jiang and H. X. Ju, *Anal. Chem.*, 2007, **79**, 6690–6696.
8 Y. Yamakoshi, N. Umezawa, A. Ryu, K. Arakane, N. Miyata, Y. Goda, T. Masumizu and T. Nagano, *J. Am. Chem. Soc.*, 2003, **125**, 12803–12809.
9 (*a*) D. Tang and J. Ren, *Anal. Chem.*, 2008, **80**, 8064–8070; (*b*) V. Mani, B. V. Chikkaveeraiah, V. Patel, J. S. Gutkind and J. F. Rusling, *ACS Nano*, 2009, **3**, 585–594.
10 S. Ishigami, S. Natsugoe, S. Hokita, X. M. Che, K. Tokuda, A. Nakajo and H. Iwashige, *J. Clin. Gastroenterol.*, 2001, **1**, 41–44.